




Article

Comfort Analysis of Hafnium (Hf) Doped ZnO Coated Self-Cleaning Glazing for Energy-Efficient Fenestration Application

Srijita Nundy¹, Aritra Ghosh^{1,*} , Abdelhakim Mesloub² , Emad Noaime²  and Mabrouk Touahmia³

¹ College of Engineering, Mathematics and Physical Sciences, Renewable Energy, University of Exeter, Penryn TR10 9FE, UK; s.nundy@exeter.ac.uk

² Department of Architectural Engineering, Ha'il University, Ha'il 2440, Saudi Arabia; a.maslub@uoh.edu.sa (A.M.); e.noaime@uoh.edu.sa (E.N.)

³ Department of Civil Engineering, Ha'il University, Ha'il 2440, Saudi Arabia; m.touahmia@uoh.edu.sa

* Correspondence: a.ghosh@exeter.ac.uk

Abstract: To attain a comfortable building interior, building windows play a crucial role. Because of the transparent nature of the window, it allows heat loss and gain and daylight. Thus, they are one of the most crucial parts of the building envelope that have a significant contribution to the overall building energy consumption. The presence of dust particles on a window can change the entering light spectrum and creates viewing issues. Thus, self-cleaning glazing is now one of the most interesting research topics. However, aside from the self-cleaning properties, there are other properties that are nominated as glazing factors and are imperative for considering self-cleaning glazing materials. In this work, for the first time, Hf-doped ZnO was investigated as self-cleaning glazing and its glazing factors were evaluated. These outcomes show that the various percentages of ZnO doping with Hf improved the glazing factors, making it a suitable glazing candidate for the cold-dominated climate.



Citation: Nundy, S.; Ghosh, A.; Mesloub, A.; Noaime, E.; Touahmia, M. Comfort Analysis of Hafnium (Hf) Doped ZnO Coated Self-Cleaning Glazing for Energy-Efficient Fenestration Application. *Materials* **2022**, *15*, 4934. <https://doi.org/10.3390/ma15144934>

Academic Editor: Andrei Victor Sandu

Received: 22 June 2022

Accepted: 13 July 2022

Published: 15 July 2022

Publisher's Note: MDPI stays neutral with regard to jurisdictional claims in published maps and institutional affiliations.



Copyright: © 2022 by the authors. Licensee MDPI, Basel, Switzerland. This article is an open access article distributed under the terms and conditions of the Creative Commons Attribution (CC BY) license (<https://creativecommons.org/licenses/by/4.0/>).

Keywords: glazing; Hf-ZnO; building; g-value; U-value; glare; thermal comfort; visual comfort; CCT; CRI

1. Introduction

Currently, buildings consume 40% of energy globally, which is due to the heating, ventilation and air conditioning load. This consumption has an adverse impact on the environment [1]. According to United Nations, migration from rural to urban areas is alarming and increasing every day. This urban influx also increases modern buildings' energy consumption to maintain indoor comfort facilities [2–4]. Buildings generally consume high levels of energy due to their poorly thermally insulated envelopes [5]. Compared to other portions of envelopes, windows are critical, as they are the only parts of the building envelope that maintain the connection between the building's interior and the exterior and allow daylight to penetrate [6].

The glazing sector is predominantly controlled by antireflection, self-cleaning and energy-saving, which are the key three principal functions [7]. For a hot climate, reflecting the solar heat or more precisely reflecting the NIR and IR part of the solar spectrum is the most strategic decision, which in turn reduces the air conditioning load [8,9]. However, antireflection is not suitable for cold climates as it is essential for the reflecting solar spectrum to be transmitted through the window to enhance the room temperature [10,11]. Hence, there is a trend now of replacing the traditional single- and double-glazed windows with advanced technology such as smart switchable EC [12], SPD [13–16], PDLC [17], thermally activated PCM [18], hydrogel [19,20], aerogel [21] or vacuum [22,23] filled windows.

The self-cleaning type of window is another class or area that can be applied to any type of building window (e.g., traditional and smart). Atmospheric pollutants possess significant

viewing challenges for window glazing. Dust includes emissions from agriculture and industry, bird droppings, pollen, mineral dust in a dry area, fibers, sand and clay [24]. Daylight transmission into buildings is affected by the deposition of atmospheric pollutants on glazing [25]. Even in a clean UK climate, building windows suffer from dust [26]. Thus, a cleaned window is indispensable for a sustainable building. Depending on the particle diameter, they either fall from the glass surface or stick on the surface. Even though the glass surface looks smooth, it has microscopically small pocks which enhance the attraction of dirt [27–29]. A self-cleaning glazing or window is a thin self-cleaning coating of film on the external surface of the glass, which protects it from dirt [30]. Generally, two types of self-cleaning technologies are available: hydrophobic and hydrophilic. Self-cleaning glazing is capable of cleaning its own surface. For self-cleaning coating, transparency is essential, as it should not create any obstacles to indoor viewing. In addition, long-term durability is crucial for cost-effectiveness.

In the past, several self-cleaning materials have been investigated particularly for photovoltaic applications [31,32] and window [33,34] applications. Zinc oxide (ZnO) is one of the most bio-friendly important semiconductors that have been investigated for self-cleaning applications. A superhydrophobic ZnO nanorods@cellulose membrane for efficient building radiative cooling was investigated [35]. ZnO-coated transparent wood was employed for building applications previously and showed 17% energy saving compared to a traditional window [36]. In another work, a ZnO nanoparticle enhanced paraffin-filled window was investigated for double glazing which showed improved efficiency [37]. To further enhance the ZnO properties, Dy₂WO₆-doped ZnO [38], Sm₃₊-doped ZnO [39] and Hf-doped ZnO [40] have been investigated for self-cleaning. ZnO for self-cleaning is one of the most popular approaches [41].

Because of the similar ionic radii, Hf-doped ZnO has potential. Transition metal ion doping enhances the surface oxygen vacancies, which improves the self-cleaning behavior. The inclusion of lower-concentration hafnium increases oxygen vacancy defects and produces hydrophilic surfaces. Previously, hafnium oxide (HfO₂) was prepared by electron beam evaporation, and three layers of HfO₂/Ag/HfO₂ showed heat mirror properties for energy-efficient window application [42]. We previously developed morphologically varied ZnO for self-cleaning application [43] and synthesized high-quality Hf-ZnO thin films with various Hf contents [40]. However, the suitability of ZnO in terms of glazing for building window applications has not yet been investigated.

How a new material will behave as a building window can be understood by analyzing its thermal and visual comfort parameters [44,45]. The solar heat gain coefficient or solar factor is one of the major influential factors that determine the indoor room temperature and thus define the thermal comfort level [46]. Most often occupants prefer a 20 °C temperature in indoor conditions [47,48]. For a cold climate, a higher solar factor is essential as it increases the room temperature and maintains a comfortable level, whereas for a hot climate, the solar factor should be limited or rejected to limit the increase in room temperature [49,50]. Visual comfort includes both the illuminance level and the color properties. Bright ambient daylight is paramount for cognitive work [51]. However, this amount should not exceed a certain level, or else discomfort glare will dominate. External daylight transmitted through the window glazing attains wavelength changes, which can create discomfort for occupants [52–54]. Color property analysis tackles these challenges.

In this work, for the first time, Hf-doped ZnO was investigated for glazing application. Thus, to understand its suitability as a future self-cleaning fenestration, glazing factor and thermal and visual comfort analyses are essential. Employing the measured transmission spectrum of different Hf-doped ZnO, essential glazing factors such as solar and luminous transmission, solar material protection factor (SMPF) and solar skin protection factors (SSPFs) have been calculated. For thermal comfort analysis, the solar factor has been evaluated. Further, correlated color temperature (CCT), color rendering index (CRI) and glare have also been calculated to understand the visual comfort and suitability of this material for building fenestration application.

2. Experiments

2.1. Materials Fabrication for Glazing

The material for the self-cleaning glazing purpose was developed using hafnium IV chloride (HfCl_4), propanol ($\text{C}_2\text{H}_5\text{OH}$), triethanolamine ($\text{C}_6\text{H}_{15}\text{NO}_3$) and zinc acetate ($\text{Zn}(\text{CH}_3\text{COOH})_2 \cdot 2\text{H}_2\text{O}$), which were purchased from Sigma Aldrich (St. Louis, MI, USA) and used without any further purification. Pure and Hf-doped ZnO were synthesized using the sol-gel synthesis method with Hf concentrations varying from 0 to 15%. Briefly, 2.2 g of $\text{Zn}(\text{CH}_3\text{COOH})_2 \cdot 2\text{H}_2\text{O}$ was made to dissolve completely in 10 mL of $\text{C}_2\text{H}_5\text{OH}$. Then, $\text{C}_6\text{H}_{15}\text{NO}_3$ was carefully poured into the above-prepared solution, where the molar ratio of triethanolamine:zinc acetate was kept at 3:5. The resultant mixture was maintained at room temperature for 5 min. Part of this sol was directly taken for preparation of pure ZnO, and the rest was separated into batches, wherein a particular amount of HfCl_4 was added, and stirred at 90°C for 1 h, thereby forming the sol for Hf-doped ZnO. These as-prepared sols were taken for the thin-film coating on glass substrates, via spin coating (Ossila spin coater, Sheffield, UK), carried out at 500 rpm for 30 s. The as-deposited thin films were taken for annealing in a muffle furnace at 350°C for 2 h. Finally, the pure and Hf-doped ZnO thin films on glass substrates were obtained after cooling down to room temperature and were further taken for characterization and application purposes. Figure 1 shows the schematic representation of different involved steps for the synthesis of the material.

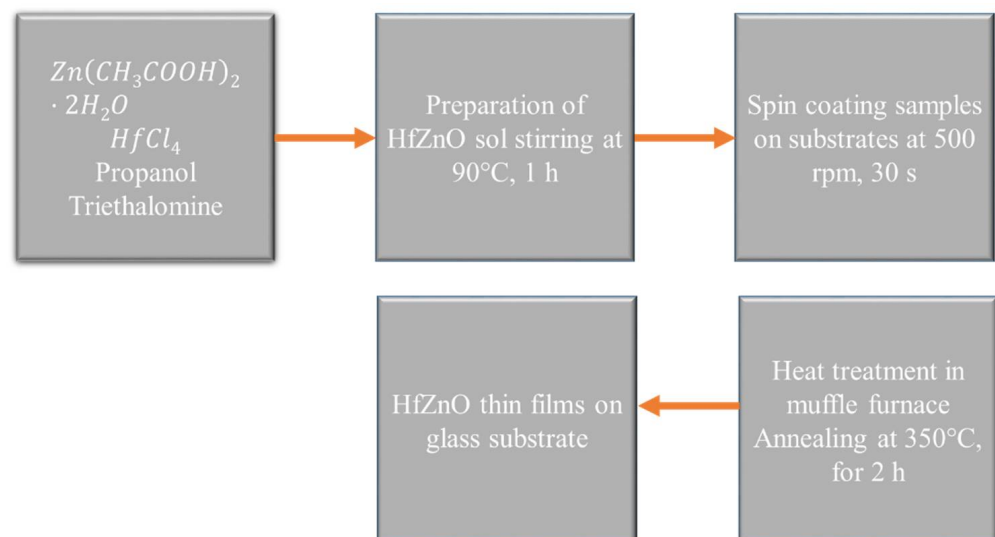


Figure 1. Schematic illustration of involved steps for synthesis of hafnium-doped ZnO.

2.2. Optical Characterization

For optical characterization of the developed glazing, a PerkinElmer Lambda 1050 spectrometer (Waltham, MA, USA) which could measure the visible and NIR transmission and reflection was employed. This system had a 150 nm diameter-based integrating sphere, and measurement was carried out at 10 nm intervals.

3. Methods

3.1. Glazing Factor Evaluation

Solar and luminous transmittance was evaluated by employing Equations (1) and (2), respectively. $T(\lambda)$ is the spectral transmission of glazing. The relative spectral distribution of the illuminant is D_{65} , $S(\lambda)$ is the relative spectral distribution of solar radiation, $V(\lambda)$ is the spectral luminous efficiency of a standard photopic observer, and wavelength interval is represented by $\Delta\lambda$.

Protection factors are crucial building window parameters that show the ability of a window to protect the building material and human skin (located behind the window) when they are exposed to solar radiation [55]. The solar material protection factor (SMPF)

is associated with the protection of building material, and the solar skin protection factor (*SSPF*) is associated with the human skin [56]. *SMPF* and *SSPF* both vary between 0 and 1 [57]. Values close to 0 indicate a low protection level, whereas close to 1 indicate a high protection level. *SMPF* and *SSPF* are represented by Equations (3) and (4).

Solar transmission

$$\tau_s = \frac{\sum_{\lambda=300 \text{ nm}}^{2500 \text{ nm}} S(\lambda)T(\lambda, \alpha)\Delta\lambda}{\sum_{\lambda=300 \text{ nm}}^{2500 \text{ nm}} S(\lambda)\Delta\lambda} \quad (1)$$

Luminous transmission

$$\tau_v = \frac{\sum_{\lambda=380 \text{ nm}}^{780 \text{ nm}} D_{65}(\lambda)T(\lambda, \alpha)V(\lambda)\Delta\lambda}{\sum_{\lambda=380 \text{ nm}}^{780 \text{ nm}} D_{65}(\lambda)V(\lambda)\Delta\lambda} \quad (2)$$

Solar material protection factor (*SMRF*)

$$SMRF = 1 - \frac{\sum_{\lambda=300 \text{ nm}}^{600 \text{ nm}} T(\lambda)C_\lambda S_\lambda \Delta\lambda}{\sum_{\lambda=300 \text{ nm}}^{600 \text{ nm}} C_\lambda S_\lambda \Delta\lambda} \quad (3)$$

where $C_\lambda = e^{-0.012\lambda}$.

Solar skin protection factor (*SSPF*)

$$SSPF = 1 - \frac{\sum_{\lambda=300 \text{ nm}}^{400 \text{ nm}} T(\lambda)E_\lambda S_\lambda \Delta\lambda}{\sum_{\lambda=300 \text{ nm}}^{400 \text{ nm}} E_\lambda S_\lambda \Delta\lambda} \quad (4)$$

E_λ is the CIE erythemal effectiveness spectrum.

3.2. Thermal Comfort

The amount of solar energy transmitted through the transparent and semitransparent part of the window is represented by the solar heat gain coefficient or solar factor (g). This includes entering infrared radiation into a building's interior and solar transmittance [55,57].

$$\begin{aligned} g &= \tau_s + q_i = \tau_s + \alpha \frac{h_i}{h_i + h_e} \\ &= \tau_s + (1 - \tau_s - \rho_s) \frac{h_i}{h_i + h_e} \end{aligned} \quad (5)$$

where h_e and h_i are the external and internal heat transfer coefficients.

3.3. Visual Comfort

Quality and quantity of light in indoor conditions are essential to understanding and analyzing visual comfort. Correlated color temperature (*CCT*) and color rendering index (*CRI*) both indicate the quality of indoor daylight [58]. Compared to external daylight, *CRI* shows the rendering ability of the incoming daylight. *CCT* is measured in kelvin (*K*) and signifies a light source's "coolness" and "warmth". *CRI* over 80 is accepted for building window application, and *CRI* over 90 is outstanding [59–61]. For *CCT*, the range between 3000 K and 7500 K is desired for transmitted daylight.

CCT was calculated from McKamy's equation [62].

$$CCT = 449n^3 + 3525n^2 + 6823.3n + 5520.33 \quad (6)$$

where $n = \frac{(x - 0.3320)}{(0.1858 - y)}$ and x and y are chromaticity coordinates.

The color rendering index (CRI) is given by

$$CRI = \frac{1}{8} \sum_{i=1}^8 R_i \quad (7)$$

The total distortion ΔE_i is determined from

$$\Delta E_i = \sqrt{(U_{t,i}^* - U_{r,i}^*)^2 + (V_{t,i}^* - V_{r,i}^*)^2 + (W_{t,i}^* - W_{r,i}^*)^2} \quad (8)$$

The special color rendering index R_i for each color sample is given by

$$R_i = 100 - 4.6\Delta E_i \quad (9)$$

To understand the quality of the indoor light, daylight glare evaluation is essential; daylight glare was evaluated in this work by employing glare subjective rating (SR) (as shown in Equation (10)) [63]. Minimum engagement of photosensors makes this method widely available and useful because it saves time and cost [64]. Theoretically, glare control potential using this glazing was identified from measured outdoor illuminance on a vertical plane as shown in Figure 2. This SR index allows the estimation of discomfort glare experienced by subjects when working at a visual daylight task (VDT) placed against a window of high or non-uniform luminance.

$$SR = 0.1909E_v^{0.31} \quad (10)$$

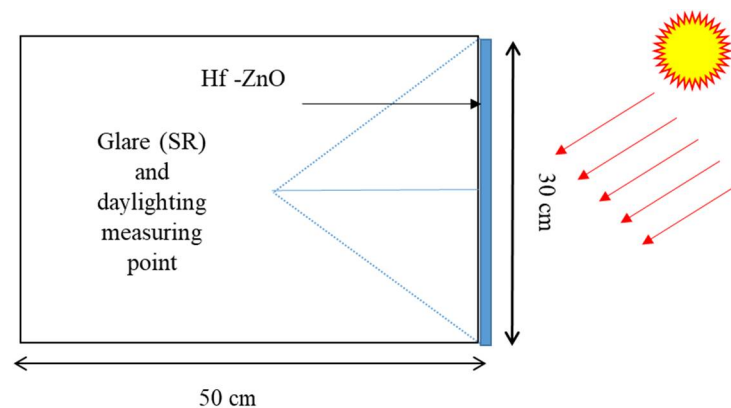


Figure 2. Schematic cross-section of a room with perovskite glazing mounted on vertical south facade.

SR for a typical sunny day in the cold-dominated climate of Penryn, UK (50.16° N, 5.10° W), was examined. Vertically south-facing Hf-doped ZnO glazing having dimensions of $30 \times 30 \times 0.5$ ($l \times w \times h$) cm in the scale model was considered, as shown in Figure 2. This large area resembles self-cleaning glazing as a large facade, while the internal surface was painted in white color with a reflectance of 0.8 [65]. Internal vertical illuminance (E_v) facing the window (worst case) was measured at the center of the room. Table 1 displays the criterion scale of SR. This method also allows the non-intrusive measuring equipment necessary for scale model daylighting assessments [66,67].

Table 1. Criterion scale of discomfort glare subjective rating (SR) [63].

Comfort Level Indicator	Glare Subjective Rating (SR)
Just intolerable	2.5
Just disturbing	1.5
Just noticeable/acceptable	0.5

4. Results

4.1. Optical Transmission

Figure 3a shows the spectral transmission of various Hf-doped ZnO for the wavelength range between 250 and 2500 nm. Transmission dropped for 15% Hf doping, while the highest transmission was observed for 6% Hf doping. The product of the spectral luminous efficiency for photopic vision $V(\lambda)$ and relative spectral distribution of illuminant D65(λ) has been included for comparison; it varied from 400 nm to 700 nm, having its peak at 555 nm. Figure 3b shows the comparison of single value solar and visible transmission for pure and different Hf-doped ZnO. Pure ZnO showed 87% solar transmission, while 3%, 6%, 9%, 12% and 15% showed 87%, 99%, 88%, 86% and 73%, respectively. Extraordinary changes occurred while the Hf doping percentage was 6%. Visible transmissions for pure and different Hf-doped ZnO are 75% (pure), 88% (3%), 93% (6%), 69% (9%), 91% (12%) and 39% (15%).

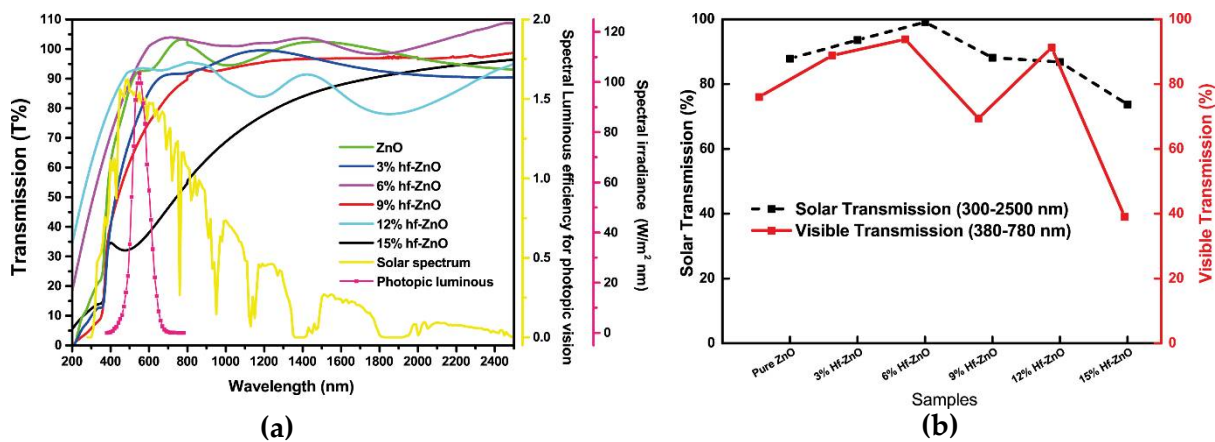


Figure 3. (a) Wavelength-dependent UV, visible and NIR transmission spectra of pure and Hf-doped ZnO thin films. (b) Relation between solar and visible transmission for ZnO with various levels of Hf doping.

Figure 4 illustrates the solar material protection factor and skin protection factor for pure and different Hf-doped ZnO. The material protection factor was higher for 15% Hf-doped ZnO, which was the reason for its lower transmission. Less solar transmission indicates lower degradation. The skin protection factor was lowest for the 12% Hf-doped ZnO, which was due to its highest transmission.

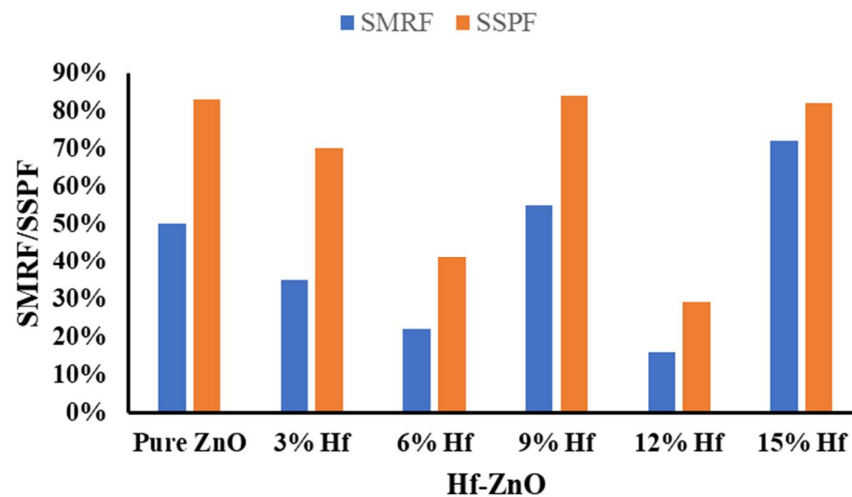


Figure 4. Solar material protection factor (SMRF) and solar skin protection factor (SSPF) for pure and different Hf-doped ZnO.

4.2. Comfort Analysis

Figure 5 illustrates the solar factor for self-cleaning glazing based on different Hf-doped ZnO. The solar factor is a crucial element for building glazing as its presence is highly recommended for a cold climate, whereas its rejection is essential for a hot climate. In this work, 6% Hf-doped ZnO showed the best solar factor for the cold-dominated climate. However, if this glazing is adopted in a heat-dominated climate, 15% Hf-doped ZnO should be selected. High values of solar factors indicate that the reflection of solar radiation from these glazings is minimal. This is also aesthetic as high reflection can cause issues for the other building users.

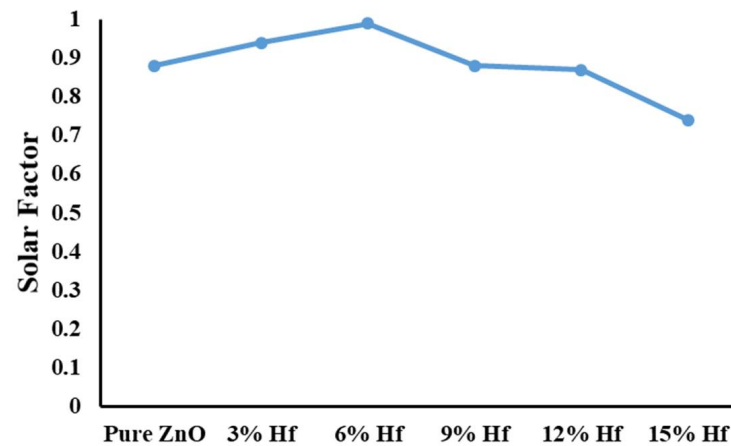


Figure 5. Solar factor for self-cleaning glazing based on different Hf-doped ZnO.

Color properties, including CCT and CRI, were calculated for Hf-ZnO glazing using Equations (6) (CCT) and (7) (CRI) and are shown in Figure 6. The 12% Hf-doped ZnO had the best CRI (>98) and CCT (>6200). Interestingly all the doped ZnO samples had higher CRI than the pure ZnO. These values satisfy the acceptance level for the comfort level criteria as prescribed in CIE CIR [68,69] and IES TM 30–15 [70]. In addition, it can be proposed that CRI and CCTs are not dependent on a single transmittance value, but their dependency relies on the overall spectrum range. A very similar outcome was previously demonstrated for other types of glazing [71,72].

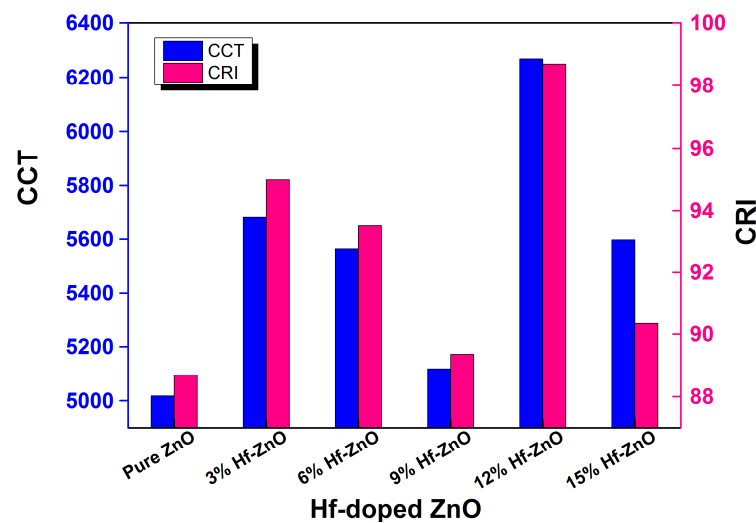


Figure 6. Color rendering index (CRI) and correlated color temperature (CCT) of pure and Hf-doped ZnO thin films.

Figure 7 shows the SR for different Hf-doped ZnO and pure ZnO-based glazing for a vertical south-facing large glazed facade located in cold-dominated climate of Penryn, in the southwest of the UK. A typical clear sunny day was considered for this analysis. The location of the subject is shown in Figure 2. It is clear from the figure that except for the 15% Hf-doped ZnO, others were not able to maintain the glare. This is definitely due to the high transmission rate for all the different Hf-doped and pure ZnO-based glazings. For a cold climatic country where the heating load is high, this penetration of higher solar light could be beneficial from a thermal comfort point of view, although visual comfort may be compromised. However, this argument is true for any type of window for which it is not possible to attain visual and thermal comfort concomitantly. The promising factor for this type of coating is a high transmission, which is key for any self-cleaning material. Transmission reduction on a double glass due to self-cleaning coating is not at all acceptable. Except for building windows, this analysis also strongly recommended the use of this material for self-cleaning coating for the PV system as no transmission reduction is attained and mostly very high transmission was achieved, particularly for the 3%, 6% and 12% Hf-doped ZnO.

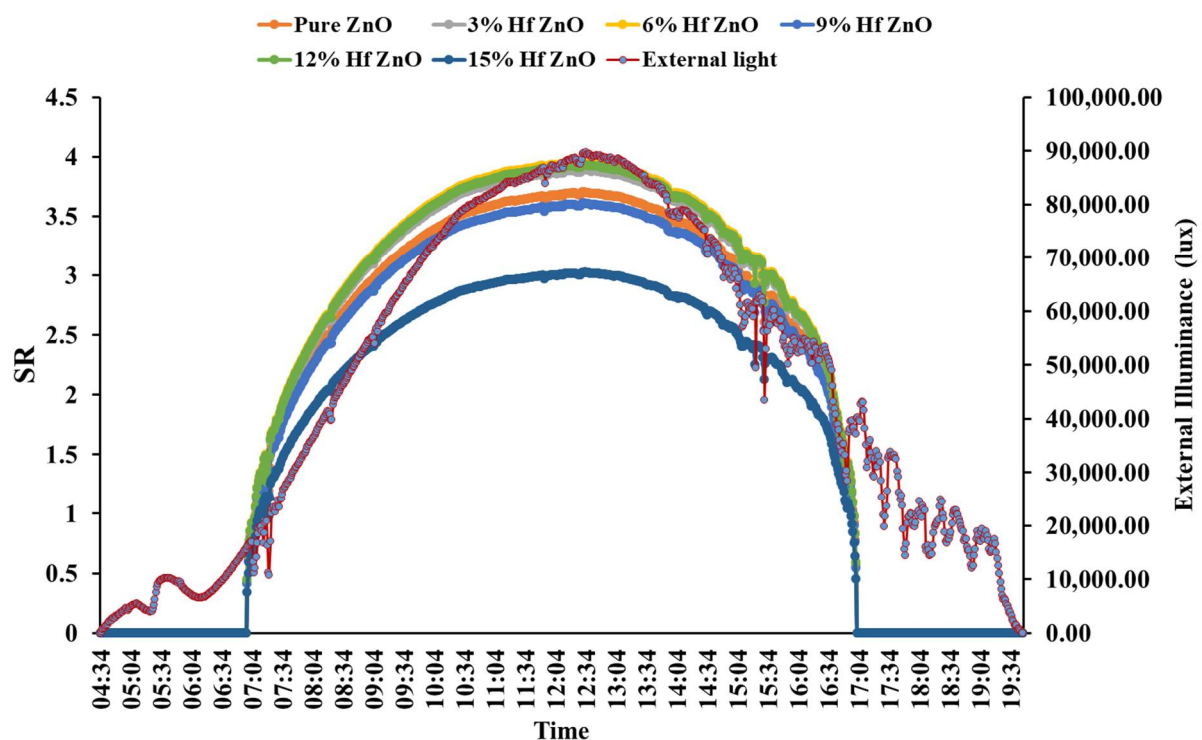


Figure 7. Glare (subjective rating) for pure and different Hf-doped ZnO.

5. Conclusions

In this work, glazing factors and thermal and visual comfort analyses of a self-cleaning coated glazing were examined. This particular self-cleaning coating was developed by the sol-gel method with the introduction of 3%, 6%, 9%, 12% and 15% Hf doping of ZnO. Results of these doped ZnO samples were also compared with pure ZnO. The visible transmission was always higher for the 6% doped ZnO. The protection factor had no trend with an increase in Hf doping. The lowest protection factor was observed at 12% Hf doping. CRI's threshold value of 80 was achieved for all the Hf-doped ZnO type glazings. A higher amount of solar factor also makes this glazing suitable for cold-dominated climates. This high solar factor also indicates that the glazing possesses lower reflection. The 15% doped ZnO showed an allowable SR limit compared to other doped ZnO samples. This was due to the lowest transmission level at the visible wavelength for 15% doped ZnO. This self-cleaning glazing can be a solution for future energy-efficient window applications.

Particularly for cold climate conditions, this self-cleaning can be a good candidate for building window application because of its high solar and visible transmission and high solar factor. In addition, because of lower reflection, it can also be applied on top of photovoltaic systems to diminish the soiling issues. In the future, further investigation is required to understand the reliability of this coating under real weather conditions after long-term outdoor exposure (following different Köppen climatic conditions).

Author Contributions: Conceptualization, S.N. and A.G.; methodology, S.N. and A.G.; software, S.N., A.G., A.M., E.N. and M.T.; validation, S.N., A.G., A.M., E.N. and M.T.; formal analysis, S.N.; investigation, A.G.; resources, S.N., A.G., A.M., E.N. and M.T.; data curation, S.N. and A.G.; writing—original draft preparation, S.N. and A.G.; writing—review and editing, S.N., A.G., A.M., E.N. and M.T. visualization, S.N., A.G., A.M., E.N. and M.T. supervision, A.G.; project administration, A.G. and A.M.; funding acquisition, A.G. and A.M. All authors have read and agreed to the published version of the manuscript.

Funding: This research has been funded by the Scientific Research Deanship at the University of Ha'il, Saudi Arabia, through project number RG-21 029.

Institutional Review Board Statement: Not applicable.

Informed Consent Statement: Not applicable.

Data Availability Statement: Not applicable.

Conflicts of Interest: The authors declare no conflict of interest.

References

1. Nundy, S.; Ghosh, A. Thermal and visual comfort analysis of adaptive vacuum integrated switchable suspended particle device window for temperate climate. *Renew. Energy* **2020**, *156*, 1361–1372. [[CrossRef](#)]
2. Nematchoua Modeste Kameni; Sadeghi, M.; Reiter, S. Strategies and scenarios to reduce energy consumption and CO2 emission in the urban, rural and sustainable neighbourhoods. *Sustain. Cities Soc.* **2021**, *72*, 103053. [[CrossRef](#)]
3. Shi, G.; Lu, X.; Zhang, H.; Zheng, H.; Zhang, Z.; Chen, S.; Xing, J.; Wang, S. Environmental Science and Ecotechnology Air pollutant emissions induced by rural-to-urban migration during China 's urbanization (2005–2015). *Environ. Sci. Ecotechnol.* **2022**, *10*, 100166. [[CrossRef](#)]
4. Yuan, R.; Rodrigues, J.F.D.; Wang, J.; Tukker, A.; Behrens, P. A global overview of developments of urban and rural household GHG footprints from 2005 to 2015. *Sci. Total Environ.* **2022**, *806*, 150695. [[CrossRef](#)] [[PubMed](#)]
5. Ghosh, A. Fenestration integrated BIPV (FIPV): A review. *Sol. Energy* **2022**, *237*, 213–230. [[CrossRef](#)]
6. Vasquez, N.G.; Rupp, R.F.; Andersen, R.K.; Toftum, J. Occupants' responses to window views, daylighting and lighting in buildings: A critical review. *Build. Environ.* **2022**, *219*, 109172. [[CrossRef](#)]
7. Garlisi, C.; Trepici, E.; Li, X.; Al, R.; Al-ali, K.; Pereira, R.; Zheng, L.; Azar, E.; Palmisano, G. Multilayer thin film structures for multifunctional glass: Self-cleaning, antireflective and energy-saving properties. *Appl. Energy* **2020**, *264*, 114697. [[CrossRef](#)]
8. Musa, A.; Hakim, M.L.; Alam, T.; Islam, M.T.; Alshammari, A.S.; Mat, K.; Salaheldeen, M.M.; Almalki, S.H.A. Polarization Independent Metamaterial Absorber with Anti-Reflection Coating Nanoarchitectonics for Visible and Infrared Window Applications. *Materials* **2022**, *15*, 3733. [[CrossRef](#)]
9. Jahid, A.; Wang, J.; Zhang, E.; Duan, Q.; Feng, Y. Energy savings potential of reversible photothermal windows with near infrared-selective plasmonic nanofilms. *Energy Convers. Manag.* **2022**, *263*, 115705. [[CrossRef](#)]
10. Mesloub, A.; Ghosh, A. Daylighting performance of light shelf photovoltaics (LSPV) for office buildings in hot desert-like regions. *Appl. Sci.* **2020**, *10*, 7959. [[CrossRef](#)]
11. Mesloub, A.; Ghosh, A.; Touahmia, M. Performance Analysis of Photovoltaic Integrated Shading Devices (PVSDs) and Semi-Transparent Photovoltaic (STPV) Devices Retrofitted to a Prototype Office Building in a Hot Desert Climate. *Sustainability* **2020**, *12*, 10145. [[CrossRef](#)]
12. Chidubem Iluyemi, D.; Nundy, S.; Shaik, S.; Tahir, A.; Ghosh, A. Building energy analysis using EC and PDLC based smart switchable window in Oman. *Sol. Energy* **2022**, *237*, 301–312. [[CrossRef](#)]
13. Mesloub, A.; Ghosh, A.; Touahmia, M.; Abdullah, G.; Alsolami, B.M.; Ahriz, A. Assessment of the overall energy performance of an SPD smart window in a hot desert climate The International Commission on Illumination. *Energy* **2022**, *252*, 124073. [[CrossRef](#)]
14. Ghosh, A.; Norton, B. Durability of switching behaviour after outdoor exposure for a suspended particle device switchable glazing. *Sol. Energy Mater. Sol. Cells* **2017**, *163*, 178–184. [[CrossRef](#)]
15. Ghosh, A.; Norton, B.; Duffy, A. Measured overall heat transfer coefficient of a suspended particle device switchable glazing. *Appl. Energy* **2015**, *159*, 362–369. [[CrossRef](#)]
16. Ghosh, A.; Norton, B.; Duffy, A. First outdoor characterisation of a PV powered suspended particle device switchable glazing. *Sol. Energy Mater. Sol. Cells* **2016**, *157*, 1–9. [[CrossRef](#)]

17. Shaik, S.; Nundy, S.; Ramana, V.; Ghosh, A.; Afzal, A. Polymer dispersed liquid crystal retrofitted smart switchable glazing: Energy saving, diurnal illumination, and CO₂ mitigation prospective. *J. Clean. Prod.* **2022**, *350*, 131444. [[CrossRef](#)]
18. Roy, A.; Ullah, H.; Ghosh, A.; Baig, H.; Sundaram, S.; Tahir, A.A.; Mallick, T.K. Understanding the Semi-Switchable Thermochromic Behavior of Mixed Halide Hybrid Perovskite Nanorods. *J. Phys. Chem. C* **2021**, *125*, 18058–18070. [[CrossRef](#)]
19. Hemaida, A.; Ghosh, A.; Sundaram, S.; Mallick, T.K. Evaluation of thermal performance for a smart switchable adaptive polymer dispersed liquid crystal (PDLC) glazing. *Sol. Energy* **2020**, *195*, 185–193. [[CrossRef](#)]
20. Hemaida, A.; Ghosh, A.; Sundaram, S.; Mallick, T.K. Simulation study for a switchable adaptive polymer dispersed liquid crystal smart window for two climate zones (Riyadh and London). *Energy Build.* **2021**, *251*, 111381. [[CrossRef](#)]
21. Ghosh, A.; Norton, B. Advances in switchable and highly insulating autonomous (self-powered) glazing systems for adaptive low energy buildings. *Renew. Energy* **2018**, *126*, 1003–1031. [[CrossRef](#)]
22. Ghosh, A.; Norton, B.; Duffy, A. Effect of atmospheric transmittance on performance of adaptive SPD-vacuum switchable glazing. *Sol. Energy Mater. Sol. Cells* **2017**, *161*, 424–431. [[CrossRef](#)]
23. Ghosh, A.; Norton, B.; Duffy, A. Effect of sky clearness index on transmission of evacuated (vacuum) glazing. *Renew. Energy* **2017**, *105*, 160–166. [[CrossRef](#)]
24. Ghosh, A. Soiling Losses: A Barrier for India's Energy Security Dependency from Photovoltaic Power. *Challenges* **2020**, *11*, 9. [[CrossRef](#)]
25. Ullah, M.B.; Kurniawan, J.T.; Poh, L.K.; Wai, T.K.; Tregenza, P.R. Attenuation of diffuse daylight due to dust deposition on glazing in a tropical urban environment. *Light. Res. Technol.* **2003**, *35*, 19–29. [[CrossRef](#)]
26. Sharples, S.; Stewart, L.; Tregenza, P.R. Glazing daylight transmittances: A field survey of windows in urban areas. *Build. Environ.* **2001**, *36*, 503–509. [[CrossRef](#)]
27. Chanchangi, Y.N.; Ghosh, A.; Baig, H.; Sundaram, S.; Mallick, T.K. Soiling on PV performance influenced by weather parameters in Northern Nigeria. *Renew. Energy* **2021**, *180*, 874–892. [[CrossRef](#)]
28. Chanchangi, Y.N.; Ghosh, A.; Sundaram, S.; Mallick, T.K. An analytical indoor experimental study on the effect of soiling on PV, focusing on dust properties and PV surface material. *Sol. Energy* **2020**, *203*, 46–68. [[CrossRef](#)]
29. Chanchangi, Y.N.; Ghosh, A.; Sundaram, S.; Mallick, T.K. Angular dependencies of soiling loss on photovoltaic performance in Nigeria. *Sol. Energy* **2021**, *225*, 108–121. [[CrossRef](#)]
30. Midtdal, K.; Jelle, B.P. Self-cleaning glazing products: A state-of-the-art review and future research pathways. *Sol. Energy Mater. Sol. Cells* **2013**, *109*, 126–141. [[CrossRef](#)]
31. Syafiq, A.; Balakrishnan, V.; Ali, M.S.; Dhoble, S.J.; Rahim, N.A.; Omar, A.; Halim, A.; Bakar, A. Application of transparent self-cleaning coating for photovoltaic panel: A review. *Curr. Opin. Chem. Eng.* **2022**, *36*, 100801. [[CrossRef](#)]
32. Adak, D.; Bhattacharyya, R.; Barshilia, H.C. A state-of-the-art review on the multifunctional self-cleaning nanostructured coatings for PV panels, CSP mirrors and related solar devices. *Renew. Sustain. Energy Rev.* **2022**, *159*, 112145. [[CrossRef](#)]
33. Roy, A.; Ghosh, A.; Mallick, T.K.; Tahir, A.A. Smart glazing thermal comfort improvement through near-infrared shielding paraffin incorporated SnO₂-Al₂O₃ composite. *Constr. Build. Mater.* **2022**, *331*, 127319. [[CrossRef](#)]
34. Ghunem, R.; Cherney, E.A.; Farzaneh, M.; Momen, G.; Illian, H.A.; Mier, G.; Peesapati, V.; Yin, F. Development and Application of Superhydrophobic Outdoor Insulation: A Review. *IEEE Trans. Dielectr. Electr. Insul.* **2022**. [[CrossRef](#)]
35. Zhao, B.; Yue, X.; Tian, Q.; Qiu, F.; Zhang, T. Controllable fabrication of ZnO nanorods @ cellulose membrane with self-cleaning and passive radiative cooling properties for building energy-saving applications. *Cellulose* **2022**, *29*, 1981–1992. [[CrossRef](#)]
36. Hu, X.; Zhang, Y.; Zhang, J.; Yang, H.; Wang, F.; Fei, B.; Noor, N. Sonochemically-coated transparent wood with ZnO: Passive radiative cooling materials for energy saving applications. *Renew. Energy* **2022**, *193*, 398–406. [[CrossRef](#)]
37. Ma, M.; Xie, M.; Ai, Q. Study on photothermal properties of Zn-ZnO/paraffin binary nanofluids as a filler for double glazing unit. *Int. J. Heat Mass Transf.* **2022**, *183*, 122173. [[CrossRef](#)]
38. Thirumalai, K.; Shanthi, M.; Swaminathan, M. Hydrothermal fabrication of natural sun light active Dy₂WO₆ doped ZnO and its enhanced photo-electrocatalytic activity and self-cleaning properties. *RSC Adv.* **2017**, *7*, 7509–7518. [[CrossRef](#)]
39. Saif, M.; Hafez, H.; Nabeel, A.I. Chemosphere Photo-induced self-cleaning and sterilizing activity of Sm³⁺ doped ZnO nanomaterials. *Chemosphere* **2013**, *90*, 840–847. [[CrossRef](#)]
40. Nundy, S.; Ghosh, A.; Tahir, A.; Mallick, T.K. Role of Hafnium Doping on Wetting Transition Tuning the Wettability Properties of ZnO and Doped Thin Films: Self-Cleaning Coating for Solar Application. *ACS Appl. Mater. Interfaces* **2021**, *13*, 25540–25552. [[CrossRef](#)]
41. El-Hossary, F.M.; Mohamed, S.H.; Noureldein, E.A.; Abo EL-Kassem, M. ZnO thin films prepared by RF plasma chemical vapour transport for self-cleaning and transparent conducting coatings. *Bull. Mater. Sci.* **2021**, *44*, 82. [[CrossRef](#)]
42. Al-Kuhaili, M.F. Optical properties of hafnium oxide thin films and their application in energy-efficient windows. *Opt. Mater.* **2004**, *27*, 383–387. [[CrossRef](#)]
43. Nundy, S.; Ghosh, A.; Mallick, T.K. Hydrophilic and Superhydrophilic Self-Cleaning Coatings by Morphologically Varying ZnO Microstructures for Photovoltaic and Glazing Applications. *ACS Omega* **2020**, *5*, 1033–1039. [[CrossRef](#)]
44. Alrashidi, H.; Ghosh, A.; Issa, W.; Sellami, N.; Mallick, T.K.; Sundaram, S. Evaluation of solar factor using spectral analysis for CdTe photovoltaic glazing. *Mater. Lett.* **2019**, *237*, 332–335. [[CrossRef](#)]
45. Ghosh, A.; Sarmah, N.; Sundaram, S.; Mallick, T.K. Numerical studies of thermal comfort for semi-transparent building integrated photovoltaic (BIPV)-vacuum glazing system. *Sol. Energy* **2019**, *190*, 608–616. [[CrossRef](#)]

46. Selvaraj, P.; Ghosh, A.; Mallick, T.K.; Sundaram, S. Investigation of semi-transparent dye-sensitized solar cells for fenestration integration. *Renew. Energy* **2019**, *141*, 516–525. [[CrossRef](#)]
47. Ghosh, A.; Norton, B.; Duffy, A. Behaviour of a SPD switchable glazing in an outdoor test cell with heat removal under varying weather conditions. *Appl. Energy* **2016**, *180*, 695–706. [[CrossRef](#)]
48. Ghosh, A. Potential of building integrated and attached/applied photovoltaic (BIPV/BAPV) for adaptive less energy-hungry building's skin: A comprehensive Review. *J. Clean. Prod.* **2020**, *276*, 123343. [[CrossRef](#)]
49. Nundy, S.; Ghosh, A.; Mesloub, A.; Abdullah, G.; Mashary, M. Impact of COVID-19 pandemic on socio-economic, energy-environment and transport sector globally and sustainable development goal (SDG). *J. Clean. Prod.* **2021**, *312*, 127705. [[CrossRef](#)]
50. Nundy, S.; Mesloub, A.; Alsolami, B.M.; Ghosh, A. Electrically actuated visible and near-infrared regulating switchable smart window for energy positive building: A review. *J. Clean. Prod.* **2021**, *301*, 126854. [[CrossRef](#)]
51. Ghosh, A.; Selvaraj, P.; Sundaram, S.; Mallick, T.K. The colour rendering index and correlated colour temperature of dye-sensitized solar cell for adaptive glazing application. *Sol. Energy* **2018**, *163*, 537–544. [[CrossRef](#)]
52. Ghosh, A.; Norton, B.; Duffy, A. Measured thermal & daylight performance of an evacuated glazing using an outdoor test cell. *Appl. Energy* **2016**, *177*, 196–203. [[CrossRef](#)]
53. Ghosh, A.; Norton, B.; Duffy, A. Measured thermal performance of a combined suspended particle switchable device evacuated glazing. *Appl. Energy* **2016**, *169*, 469–480. [[CrossRef](#)]
54. Ghosh, A.; Norton, B.; Duffy, A. Daylighting performance and glare calculation of a suspended particle device switchable glazing. *Sol. Energy* **2016**, *132*, 114–128. [[CrossRef](#)]
55. Jelle, B.P.; Gustavsen, A.; Nilsen, T.N.; Jacobsen, T. Solar material protection factor (SMPF) and solar skin protection factor (SSPF) for window panes and other glass structures in buildings. *Sol. Energy Mater. Sol. Cells* **2007**, *91*, 342–354. [[CrossRef](#)]
56. Grosjean, A.; Le Baron, E. Longtime solar performance estimations of low-E glass depending on local atmospheric conditions. *Sol. Energy Mater. Sol. Cells* **2022**, *240*, 111730. [[CrossRef](#)]
57. Ghosh, A.; Mallick, T.K. Evaluation of optical properties and protection factors of a PDLC switchable glazing for low energy building integration. *Sol. Energy Mater. Sol. Cells* **2017**, *176*, 391–396. [[CrossRef](#)]
58. Bhandari, S.; Ghosh, A.; Roy, A.; Kumar, T.; Sundaram, S. Compelling temperature behaviour of carbon-perovskite solar cell for fenestration at various climates. *Chem. Eng. J. Adv.* **2022**, *10*, 100267. [[CrossRef](#)]
59. Ghosh, A.; Mesloub, A.; Touahmia, M.; Ajmi, M. Visual Comfort Analysis of Semi-Transparent Perovskite Based Building Integrated Photovoltaic Window for Hot Desert. *Energies* **2021**, *14*, 1043. [[CrossRef](#)]
60. Ghosh, A.; Norton, B. Optimization of PV powered SPD switchable glazing to minimise probability of loss of power supply. *Renew. Energy* **2019**, *131*, 993–1001. [[CrossRef](#)]
61. Ghosh, A.; Sundaram, S.; Mallick, T.K. Colour properties and glazing factors evaluation of multicrystalline based semi-transparent Photovoltaic-vacuum glazing for BIPV application. *Renew. Energy* **2019**, *131*, 730–736. [[CrossRef](#)]
62. McCamy, C.S. Correlated color temperature as an explicit function of chromaticity coordinates. *Color Res. Appl.* **1992**, *17*, 142–144. [[CrossRef](#)]
63. Lee, E.S.; DiBartolomeo, D.L. Application issues for large-area electrochromic windows in commercial buildings. *Sol. Energy Mater. Sol. Cells* **2002**, *71*, 465–491. [[CrossRef](#)]
64. Ghosh, A.; Bhandari, S.; Sundaram, S.; Mallick, T.K. Carbon counter electrode mesoscopic ambient processed & characterised perovskite for adaptive BIPV fenestration. *Renew. Energy* **2020**, *145*, 2151–2158. [[CrossRef](#)]
65. Ghosh, A.; Norton, B.; Mallick, T.K. Daylight characteristics of a polymer dispersed liquid crystal switchable glazing. *Sol. Energy Mater. Sol. Cells* **2018**, *174*, 572–576. [[CrossRef](#)]
66. Sudan, M.; Tiwari, G.N. Daylighting and energy performance of a building for composite climate: An experimental study. *Alex. Eng. J.* **2016**, *55*, 3091–3100. [[CrossRef](#)]
67. Thanachareonkit, A.; Scartezzini, J.L.; Andersen, M. Comparing daylighting performance assessment of buildings in scale models and test modules. *Sol. Energy* **2005**, *79*, 168–182. [[CrossRef](#)]
68. CIE Publication. *Spectral Luminous Efficiency Functions Based upon Brightness Matching for Monochromatic Point Sources with 2° and 10° Fields*; CIE Publication: Vienna, Austria, 1988; p. 75. ISBN 3900734119.
69. CIE. *CIE 1988 2° Spectral Luminous Efficiency Function for Photopic Vision*; CIE: Vienna, Austria, 1990; Volume 2.
70. *Illuminating Engineering Society of North America* 2015.
71. Ghosh, A.; Norton, B. Interior colour rendering of daylight transmitted through a suspended particle device switchable glazing. *Sol. Energy Mater. Sol. Cells* **2017**, *163*, 218–223. [[CrossRef](#)]
72. Piccolo, A.; Pennisi, A.; Simone, F. Daylighting performance of an electrochromic window in a small scale test-cell. *Sol. Energy* **2009**, *83*, 832–844. [[CrossRef](#)]